Solving Nonlinear Differential Equations

Flavio Sartoretto and Angelo Rubino
DAIS, Università Ca' Foscari Venezia

-

Abstract

Mathematica is great in solving analytically linear differential equations. It is also a good companion for computing numerical solutions to non–linear equations. We attack the reduced–gravity, shallow–water equation (RSE) problem. We compare the analytical solution to our problem without friction to the numerical solution obtained either with Mathematica or via Matlab. We exploit Mathematica ability in solving systems of non-linear Ordinary Differential Equations, on the way to identify some analytical solution to RSE when friction is non-negligible.

1 Introduction

Geophysical frontal vortexes are frequently observed in the ocean (see, e.g., McWilliams 1985; Olson 1991). Figure 1 shows an example of such phenomena, i.e. gulf stream rings.

They are believed to play a fundamental role in different oceanic phenomena like, e.g., those related to the transfer of physical, chemical, and biological properties across frontal regions (see, e.g., Saunders 1971; Cheney et al. 1976; Armi and Zenk 1984; Joyce 1984; Olson et al. 1985; Dengler et al. 2004), to the formation and transformation of water masses (see, e.g., Gascard et al., 2002; Budeus et al., 2004), and to the downward propagation of wind generated near-inertial waves (Lee and Niiler, 1998; Zhai et al., 2007). This extraordinary large relevance explains why, in the last decades, oceanic frontal vortexes have been deeply investigated experimentally, analytically and numerically (see, e.g., Csanady, 1979; Gill, 1981; Nof, 1983; McWilliams, 1985, 1988; Rubino and Brandt 2003; Rubino et al. 2002).

Figure 2 shows sketches of typical ocean rings. In this paper, the dynamics of non-stationary, nonlinear, axisymmetric, warm-core geophysical surface frontal vortexes affected by Rayleigh friction (called also "pulsons") is semi-analytically analyzed using the nonlinear, non-stationary reduced-gravity shallow-water equations Figures 3, and 4 show the first layer of a pulson, and its cross-section, respectively.

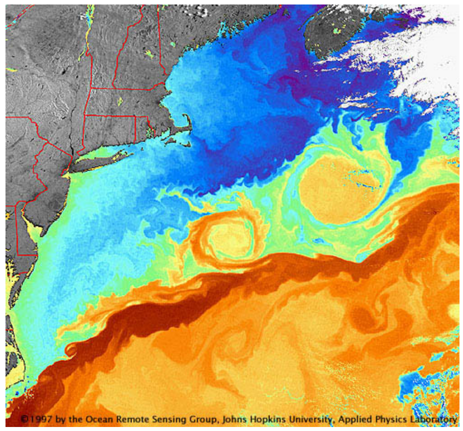

Figure 1: Satellite image of gulf stream rings.

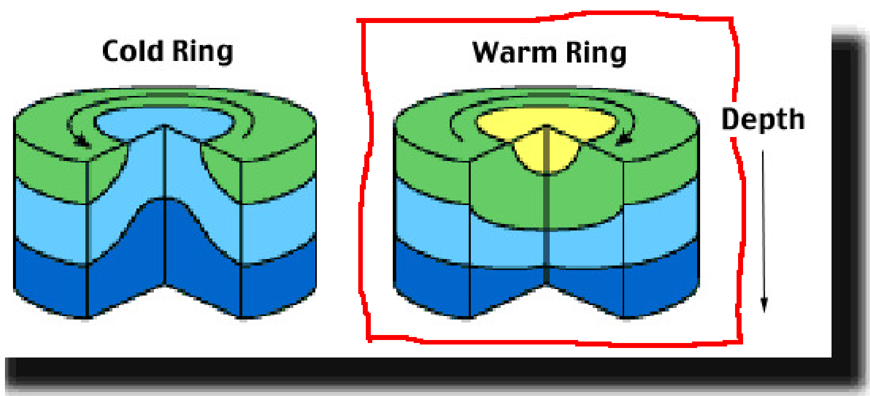

Figure 2: Ocean ring sketch.

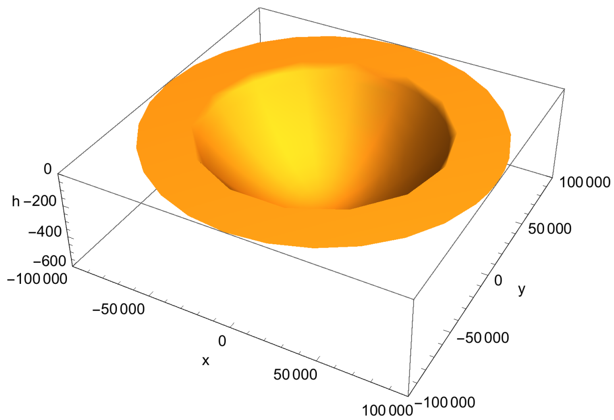

Figure 3: View of a circular pulson

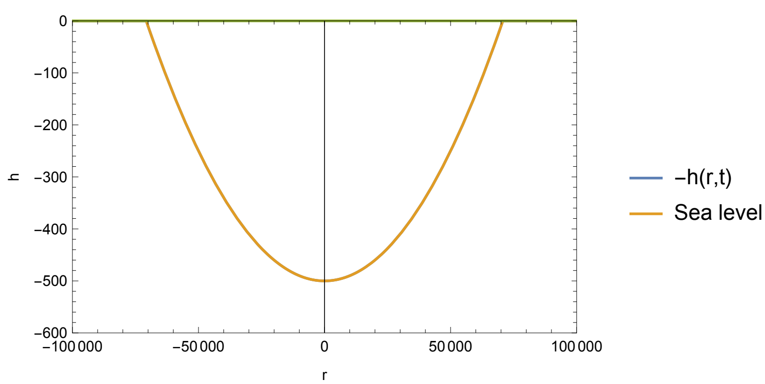

Figure 4: Cross section of a circular pulson.

2 Modeling

Assuming circular symmetry, the nonlinear, reduced–gravity, shallow-water equations for a rotating system in polar coordinates are

$$\begin{aligned}
\frac{\partial \nu_\theta}{\partial t} + \nu_r \frac{\partial \nu_\theta}{\partial r} + \frac{\nu_r\,\nu_\theta}{r} + f\,\nu_r + s\,\nu_\theta = 0, \\
\frac{\partial \nu_r}{\partial t} + \nu_r \frac{\partial \nu_r}{\partial r} + \frac{\nu_r\,\nu_\theta}{r} - \frac{\nu_\theta^2}{r} - f\,\nu_\theta + g'\,\frac{\partial h}{\partial r} + s\,\nu_r = 0, \\
\frac{\partial h}{\partial t} + \frac{\partial h \nu_r}{\partial t} + \frac{h\nu_r}{r} = 0
\end{aligned}$$

We aim at computing solutions that represent circular, frontal, warm–core eddies, displaying suitable velocity field and shape

$$\nu_\theta = -\sum_{i=1}^{n} L_i\, r^{2i-1}, \quad \nu_r = K r, \quad h = \sum_{i=0}^{2n-1} A_i\, r^{2i}.$$

By substituting the assumed velocity field and shape, when $n = 1$ we obtain the non–linear system of Ordinary Differential Equations (ODE) describing the circular *pulson*

$$\begin{aligned}
\frac{\mathrm{d}L_1}{\mathrm{d}t} + 2K\,L_1 - f\,K + s\,L_1 = 0, \\
\frac{\mathrm{d}K}{\mathrm{d}t} - L_1^2 + K^2 + f\,L_1 + 2g' A_1 + s\,K = 0, \\
\frac{\mathrm{d}A_0}{\mathrm{d}t} + 2K\,A_0 = 0, \\
\frac{\mathrm{d}A_1}{\mathrm{d}t} + 4K\,A_1 = 0.
\end{aligned}$$

Analytic solutions

$$\{K(t), L_1(t), A_0(t), A_1(t)\}$$

to this system of ODE are available when $s = 0$ (see e.g. Rubino et al. 1998), numeric solutions can be computed for any (reasonable) s value, when suitable initial conditions are set.

For a given pair of parameter values, $\bar{f}, \bar{g}'$, assume suitable, physic initial conditions $\mathcal{I}$ were set, which give a well-conditioned ODE system.

When $s = 0$, we have a P–periodic, analytic solution. $P \simeq 70{,}168$ seconds is called the "inertial period".

Figure 5 shows a plot of $\log_{10}$ of the modulus of the four components in the analytic solution of our system, for appropriate initial conditions. Note that all components of the solution are periodic, with inertial period $P \simeq 70,167$.

By using NDSolve, we can compute the corresponding numeric solution. Analytic and numeric solutions well match. For each entry $z(t)$ in the solution,

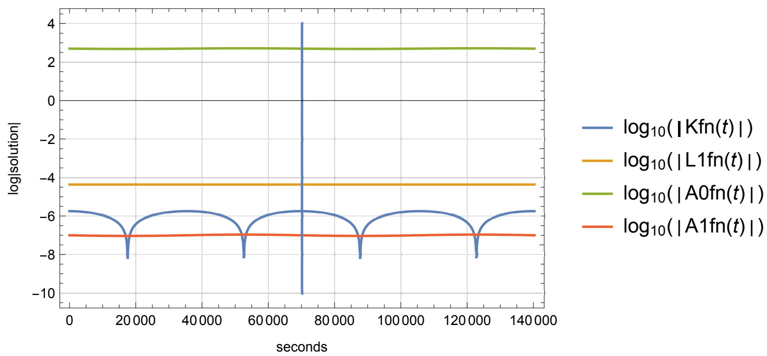

Figure 5: Plot, $\log_{10}|\text{analytic solution}|$, $s = 0$.

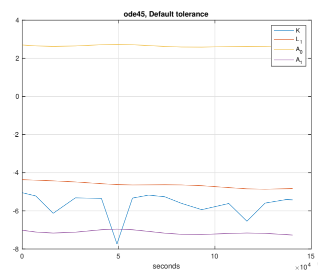

(ode45)

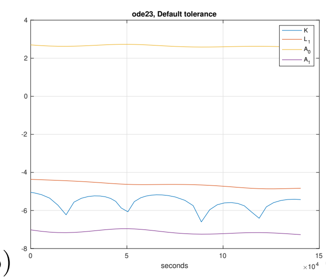

(ode23)

Figure 6: $\log_{10}$ of the modulus of the numeric solutions by Matlab ODE solvers, low (default) accuracy.

let $\tilde{z}(t)$ the corresponding numeric solution. Let us consider the L_2 error

$$e_z = \sqrt{\int_0^P (z(t) - \tilde{z}(t))^2 \, dt}.$$

The accuracy of `Mathematica` numerical solution is summarized below:

$$e_K = 2.00002 \times 10^{-9}, \quad e_{L_1} = 9.68456 \times 10^{-11},$$
$$e_{A_0} = 6.00225 \times 10^{3}, \quad e_{A_1} = 1.02564 \times 10^{-11}.$$

Using the built-in function ToMatlab, one can easily export our ODE system into a Matlab code.

Figure 6 shows plots by using two Matlab solvers, i.e. ode45 and ode23, and default package tolerances `RelTol = 1e-4`, `AbsTol = 1e-4`. The numeric solution clearly differ from the analytical solution, shown in Figure 5.

By setting lower tolerance values `RelTol = 1e-14`, `AbsTol = 1e-14`, better plots are attained, as confirmed by Figure 7.

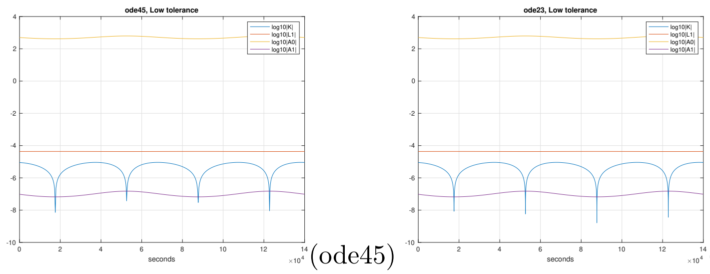

(ode45) (ode23)

Figure 7: Analogous to the previous Figure, when high accuracy is required.

`Package`	e_K	e_{L_1}	e_{A_0}	e_{A_1}
`Matlab`	`1.94e-03`	`6.70e-05`	`2.25e+04`	`8.88e-06`
`Mathematica`	`2.00e-09`	`9.68e-11`	`6.00e+03`	`1.03e-11`

Table 1: Numeric errors.

Table 1 summarizes the the L_2 errors raised by Matlab's `ode45`, when high accuracy is set, and by `Mathematica`, standard NDSolve. By inspecting the Table, one can see that Matlab `ode45` solver gives higher errors respect to `Mathematica` one.

We exploited three Matlab solvers: ode45, ode23, ode15s. Error behaviors similar to those in Table 1 were obtained.

3 Work in progress...

Let us assume now $s > 0$. Analytic solutions are not available.

For a feasible $s = 10^{-5}$ value, the numeric solution by `Mathematica` is shown by Figure 8, in the interval $0 < t < 8 \times P$.

Note that our ODE system S has four unknowns, K, L_1, A_0, A_1.

The third equation can be decoupled, hence we obtain a 3–unknowns, K, L_1, A_1, non–linear ODE system, S'. In the sequel, we deal with this reduced system.

Our computations were performed in batch–mode on a 2.30 GHz `HP ProLiant DL560 Gen8`, with 256 GB RAM.

3.1 Changing parameters

Any attempt to solve our ODE system by DSolve, when $s \neq 0$, returned unevaluated.

Let us play with parameters g', f, in order to obtain a "simpler" (non–linear) ODE system.

By setting $g' = \bar{g'} \neq 0$, $f = 0$, DSolve returns an unevaluated command.

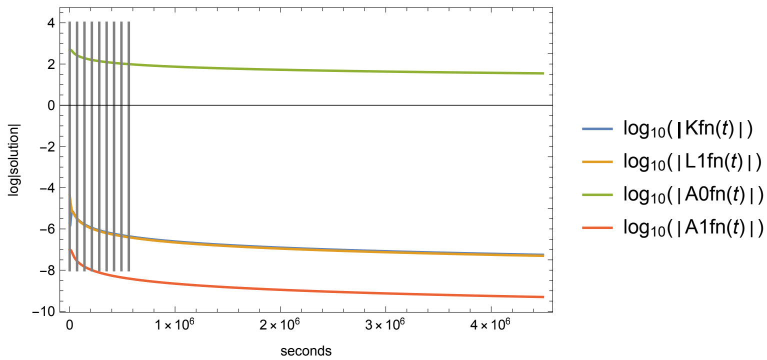

Figure 8: Non-zero friction, $\log_{10}$ of modulus `Mathematica` numeric solution.

By setting $g' = 0$, $f = \bar{f} \neq 0$, DSolve timed out.

By setting $g' = 0$, $f = 0$ values, the ensuing system S' is non-linear, and `Mathematica` finds four, complex solutions, labeled S_1, S_2, S_3, S_4, which depends upon constants C_1, C_2, C_3.

In order to compare these analytic solutions to numeric ones, we must impose our given initial conditions

$$\mathcal{I} = \{K(0) = K_0, \quad L_1(0) = L_{1,0}, \quad A_1(0) = A_{1,0}\}.$$

One must solve the conditions $\mathcal{I}$ upon C_1, C_2, C_3, by considering either solution S_1, or S_2, or S_3, or S_4.

By using Reduce on the system $\mathcal{I}$,

- when Solutions 1, 3, and 4 are considered, `False` is obtained,
- when Solution 2 is exploited, an expression is computed.

Hence we focus on Solution 2.

In the sequel, any reference to "the" solution of our ODE system, applies to S_2, and "the" system $\mathcal{I}$ is the one attached to this solution.

In order to get real components in the solution given by `Mathematica`, by careful analysis one is forced to assume $C_1 = 0$. By some (non standard, hand–made) simplifications, a solution depending upon C_2, C_3, with two real components, one pure imaginary is the best one can find. We conclude that the given analytic solution is a useless, non–physic solution, which cannot match our initial conditions.

4 Conclusions

We analyzed the accuracy of `Mathematica` and Matlab numeric solutions to a non-linear system of ODE, by comparing with a known analytic solution.

We found that `Mathematica` seems more accurate than Matlab, at least when attacking the ODE system by a naive approach.

We tried to analytically solve the non-linear system of ODE when non-zero friction is active. `Mathematica` was able to find some analytical solution to a "simple" non-linear instance. Unfortunately, such solutions have no physical significance.

Bibliography

[1] L. Armi and W. Zenk. Large lenses of highly saline mediterranean. *Water. J. Phys. Oceanogr.*, 14:1560–1575, 1984.

[2] G. Budeus, B. Cisewski, S. Ronski, and D. Dietrich. Structure and effects of a long lived vortex in the greenland sea. *Geophys. Res. Lett.*, 31:L05304, 2004.

[3] R. E. Cheney, W. H. Gemmill, and M. K. Shank. Tracking a gulf stream ring with sofar floats. *J. Phys. Oceanogr.*, 6:741–749, 1976.

[4] G. T. Csanady. The birth and death of a warm core ring. *J. Geophys. Res.*, 84:777–780, 1979.

[5] B. Cushman-Roisin. Exact analytical solutions for elliptical vortices of the shallow-water equations. *Tellus A: Dynamic Meteorology and Oceanography*, 39(3):235–244, 1987.

[6] B. Cushman-Roisin, W. H. Heil, and D. Nof. Oscillations and rotations of elliptical warm-core rings. *J. Geophys. Res.*, 90(11):756–764, 1985.

[7] B. Cushman-Roisin and S. Merchant-Both. Elliptical warm core rings in a two-layer ocean with ambient shear. *J. Phys. Oceanogr.*, 25:2011–2024, 1995.

[8] M. Dengler, F. Schott, C. Eden, P. Brandt, J. Fischer, and R. Zantopp. Break–up of the deep western boundary current into eddies at 8^os. *Nature*, 432:1018–1020, 2004.

[9] G. R. Flierl and R. P. Mied. Frictionally induced circulations and spin down of a warm-core ring. *J. Geophys. Res.*, 90:8917–8927, 1985.

[10] J. C. Gascard, A. J. Watson, M. J. Messias, K. A. Olson, T. Johannessen, and K. Simonse. Long-lived vortices as a mode of deep ventilation in the greenland sea. *Nature*, 416(6880):525–527, 2002.

[11] A. E. Gill. Homogeneous intrusions in a rotating stratified fluid. *J. Fluid Mech.*, 103:275–296, 1981.

[12] T. M. Joyce. Velocity and hydrographic structure of a warm core ring. *J. Phys. Oceanogr.*, 14:936–947, 1984.

[13] D. K. Lee and P. P. Niiler. The inertial chimney: the near-inertial drainage from the ocean surface to the deep layer. *J. Geophys. Res.*, 103:7579–7591, 1998.

[14] E. M. Mårtensson, E. D. Nilsson, G. de Leeuw, L. H. Cohen, and H.-C. Hansson. Laboratory simulations and parameterization of the primary marine aerosol production. *Journal of Geophysical Research: Atmospheres*, 108(D9), 2003.

[15] J. C. McWilliams. Sub–mesoscale coherent vortices in the oceans. *Rev. Geophys.*, 23:165–182, 1985.

[16] J. C. McWilliams. Vortex generation through balanced adjustment. *J. Phys. Oceanogr.*, 18:1178–1192, 1988.

[17] D. Nof. On the migration of isolated eddies with application to gulf stream rings. *J. Mar. Res.*, 41:399–425, 1983.

[18] D. B. Olson. Rings in the ocean. *Annu. Rev. Earth Planet. Sci.*, 19:283–311, 1991.

[19] D. B. Olson, R. W. Schmitt, M. Kennelly, and T. M. Joyce. A twolayer diagnostic model of the long–term physical evolution of warm-core ring 82b. *J. Geophys. Res.*, 90:8813–8822, 1985.

[20] A. Rubino and P. Brandt. Warm-core eddies studied by laboratory experiments and numerical modeling. *J. Phys. Oceanogr.*, 33:431–435, 2003.

[21] A. Rubino, P. Brandt, and K. Hessner. Analytical solutions for circular eddies of the reduced-gravity, shallow-water equations. *J. Phys. Oceanogr.*, 28:999–1002, 1998.

[22] A. Rubino and S. Dotsenko. The stratified pulson. *J. Phys. Oceanogr.*, 36:711–719, 2006.

[23] A. Rubino, S. Dotsenko, and P. Brandt. Nonstationary westward translation of nonlinear frontal warm–core eddies. *J. Phys. Oceanogr.*, 39(6):1486–1494, 2009.

[24] A. Rubino, K. Hessner, and P. Brandt. Decay of stable warm-core eddies in a layered frontal model. *J. Phys. Oceanogr.*, 32:188–201, 2002.

[25] I. Sachihiko, Y. Shimizu, I. Shin-ichi, and I. Yasuda. Evolution and decay of a warm-core ring within the western subarctic gyre of the north pacific, as observed by profiling floats. *J. J. Oceanogr.*, 67:281–293, 2011.

[26] P. M. Saunders. Anticyclonic eddies formed from shoreward meanders of the gulf stream. *Deep-Sea Res.*, 18:1207–1220, 1971.

[27] A. Tomosada. Generation and decay of kuroshio warm-core rings. *Deep–Sea Res.*, 33:1475–1486, 1986.

[28] X. Zhai, R. J. Greatbatch, and C. Eden. Spreading of near-inertial energy in a $1/12^o$ model of the north atlantic ocean. *Geophys. Res. Lett.*, 34:L10609, 2007.